*RevMexAA (Serie de Conferencias)*, **9**, 123–130 (2000)

# EMISSION LINE SPECTRA FROM LOW-DENSITY LABORATORY PLASMAS

P. Beiersdorfer,[1] G. V. Brown,[1] J. J. Drake,[2] M.-F. Gu,[3] S. M. Kahn,[3] J. K. Lepson,[4] D. A. Liedahl,[1] C. W. Mauche,[1] D. W. Savin,[3] S. B. Utter,[1] and B. J. Wargelin[2]

RESUMEN

Estamos realizando mediciones en el laboratorio de las líneas de emisión de iones importantes en la astrofísica, en el rango espectral de rayos-X de entre 1 y 400 Å , que cubrirán las misiones espaciales *Chandra*, *XMM*, *Astro-E* y *EUVE*. Los datos, obtenidos en un ambiente controlado a densidades similares a las de coronas estelares, son usados para verificar la exactitud y completez de códigos de modelaje espectral. Nuestro trabajo incluye la compilación de líneas de emisión de fierro, de capa L entre 6 y 18 Å y de capa M de 50 a 200 Å. Muchas líneas son identificadas por primera vez y se determinan los flujos correspondientes, faltantes en los modelos. Nuestras medidas también permiten determinar la exactitud de los cálculos de excitación de líneas, incluyendo excitación colisional, recombinación dielectrónica y excitación resonante. Estos resultados permiten calibrar casos específicos de diagnósticos de cocientes de líneas. Se dan ejemplos de datos obtenidos recientemente.

ABSTRACT

Using spectroscopic equipment optimized for laboratory astrophysics, we are performing systematic measurements of the line emission from astrophysically relevant ions in the wavelength band between 1 and 400 Å important to X-ray missions such as *Chandra*, *XMM*, *Astro-E*, and *EUVE*. Obtained in a controlled laboratory setting at electron densities similar to those found in stellar coronae, the data are used to test spectral modeling codes for accuracy and completeness. Our effort includes the compilation of the iron L-shell emission lines from 6–18 Å and the iron M-shell emission lines from 50–200 Å. Many lines have been identified for the first time, and the fluxes from lines missing in the spectral modeling codes are assessed. Our measurements also assess the accuracy of line excitation calculations, including direct electron-impact excitation, dielectronic recombination, and resonance excitation. These measurements yield a calibration of specific diagnostic line ratios. Examples of our current measurements are given.

*Key Words:* **ATOMIC DATA — ATOMIC PROCESSES — LINE: FORMATION — LINE: IDENTIFICATION**

Astrophysical Plasmas: Codes, Models, and Observations (Mexico City, 25-29 October 1999)
Editors: Jane Arthur, Nancy Brickhouse, & José Franco

## 1. INTRODUCTION

The analysis of spectral emission data from medium and high resolution X-ray and EUV satellite missions requires spectral models that are both accurate and complete. Accuracy means that the correct atomic data are used, e.g., accurate line positions, excitation and recombination cross sections, and radiative rates. Completeness means that all relevant lines and atomic processes are included in the models. To test spectral

[1]High Temperature Physics and Astrophysics Division, Lawrence Livermore National Laboratory, Livermore, CA, USA.
[2]Harvard-Smithsonian Center for Astrophysics, Cambridge, MA, USA.
[3]Department of Physics, Columbia University, New York, NY, USA.
[4]Space Sciences Laboratory, Univ. of California, Berkeley, CA, USA.

models for accuracy and completeness, comparisons with experimental data obtained in a controlled laboratory environment are needed.

Among different laboratory sources capable of producing reliable atomic data, tokamaks and electron beam ion traps (EBIT) provide spectral data in a density and temperature regime most applicable to X-ray emitting astrophysical situations. Tokamak sources have been extensively used to assess the accuracy of the atomic data related to the K-shell emission line spectra from hydrogenlike and heliumlike ions, including calculations of dielectronic recombination, collisional excitation, and radiative cascades (Beiersdorfer et al. 1989a; Bombarda et al. 1988; Decaux et al. 1991; Keenan et al. 1991; Bitter et al. 1993; Smith et al. 1993; Beiersdorfer et al. 1995). An analysis of the iron K-shell spectrum on the PLT tokamak extended such measurements to iron charge states as low as Fe XVIII, providing a very detailed line list of K-shell lines (Beiersdorfer et al. 1993). Few tokamak observations exist of astrophysically relevant L-shell x-ray spectra because these emanate from colder regions of the plasma with a correspondingly diminished diagnostic importance for magnetic fusion plasmas. An exception is the measurement of the iron L-shell emission from $n = 4 \rightarrow 2$ and $n = 5 \rightarrow 2$ transitions in Fe XXI through Fe XXIV ions on the PLT tokamak (Wargelin et al. 1998) that covered the 7 – 9 Å region. This measurement was performed with a high-resolution crystal spectrometer built specifically for measuring L-shell spectra (Beiersdorfer et al. 1989b). The measurement successfully validated spectral modeling calculations and yielded line lists with wavelength accuracies up to one part in 40,000. Tokamaks have also provided astrophysically important spectra in the extreme ultraviolet region. For example, Stratton, Moos, & Finkenthal (1984) reported line intensities for several 2-2 transitions in Fe XVIII through Fe XXIII that have been used to test emission line predictions, while Sugar & Rowan (1995) have reported very accurate wavelength measurements.

An EBIT provides a higher level of control than tokamaks for producing spectra relevant to astrophysics. The reason is that an EBIT provides almost complete control over the choice of charge states and excitation processes, as we illustrate below. As a result, many of our laboratory astrophysics investigations have involved the use of an EBIT.

In the following, we describe the Livermore EBIT facility and present recent results of our work. These include measurements of contributions from resonance excitation and dielectronic recombination satellite lines to the $3d \rightarrow 2p$ emission lines in Fe XXIV, calibration of the singlet to triplet ratio of the $3d \rightarrow 2p$ lines in neonlike ions, and line surveys in the X-ray and extreme ultraviolet region.

## 2. THE EBIT SPECTROSCOPIC SOURCE

The Livermore Electron Beam Ion Trap was specifically developed and built for studying the spectroscopic properties of highly charged ions (Levine et al. 1989). It has been in operation for over a decade during which spectroscopic measurements have been optimized to provide state-of-the-art measurements in the 1 – 7000 Å region. Special emphasis has been placed on the X-ray and EUV regions to provide laboratory data for present and future astrophysics missions such as *ASCA*, *Chandra*, *EUVE*, *DXS*, *XMM*, and *Astro-E*.

The EBIT is a modified electron beam ion source built to study the interaction of highly charged ions with an electron beam by looking directly into the trap. Magnetic fields confine and focus the electrons, which can be accelerated to any energy between about 100 eV and 200,000 eV. Neutral atoms or ions with low charge are injected into the nearly monoenergetic beam where they are collisionally ionized and excited. As the electrons pass through the trap region of 2-cm length, the beam is compressed to a diameter of approximately 60 $\mu$m by a 3-Tesla magnetic field, generated by a pair of superconducting Helmholtz coils. There, the ions are longitudinally confined by applying the appropriate voltages to a set of three drift tubes through which the beam passes. Radial confinement is provided by electrostatic attraction of the electron beam, as well as flux freezing of the ions within the magnetic field. All three drift tube voltages float on top of a potential (the common drift tube voltage) that is supplied by a low-noise high-voltage amplifier, and the electron beam energy is determined by the sum of these potentials. The electron beam density at a given beam energy can be selected by varying the beam current. It typically is in the range of $2 \times 10^{11} - 5 \times 10^{12}$ cm$^{-3}$.

Six axial slots cut in the drift tubes and aligned with six vacuum ports permit direct line-of-sight access to the trap, as shown in Figure 1. One port is used for introducing atomic or molecular gases into the trap by means of a ballistic gas injection system. The remaining five ports are used for spectroscopic measurements.

A typical arrangement for X-ray astrophysics is shown in Figure 1. A windowless high-purity Ge detector

Astrophysical Plasmas: Codes, Models, and Observations (Mexico City, 25-29 October 1999)
Editors: Jane Arthur, Nancy Brickhouse, & José Franco

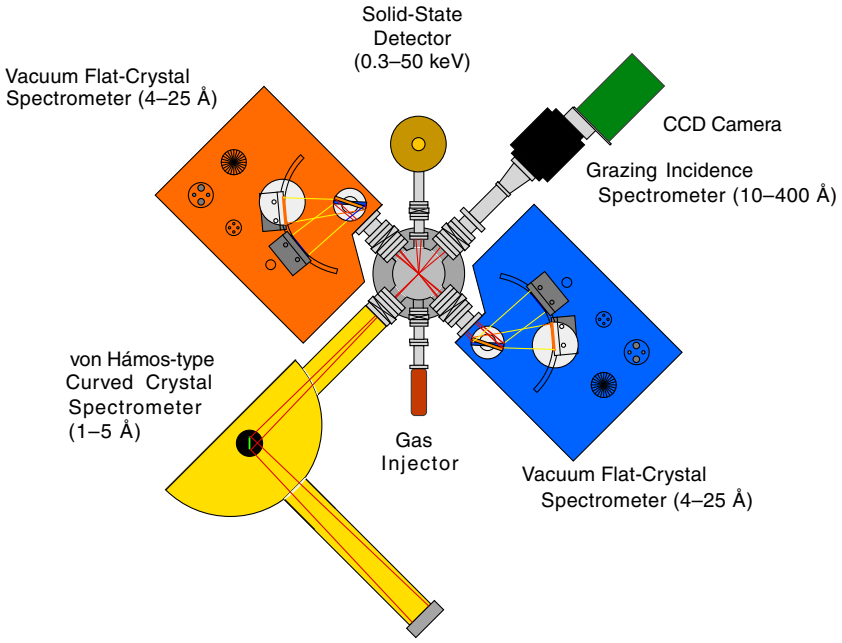


Fig. 1. Radial cut through EBIT showing the diagnostic access to the trap.

Astrophysical Plasmas: Codes, Models, and Observations (Mexico City, 25-29 October 1999)
Editors: Jane Arthur, Nancy Brickhouse, & José Franco

monitors the overall X-ray emission from the ions. This signal is used for tuning the facility, for count rate normalization, and for monitoring the presence of impurity ions. A high-resolution bent-crystal spectrometer provides detailed information on K-shell line emission spectra below 5 Å (Beiersdorfer et al. 1990). Two flat-crystal spectrometers operating *in vacuo* provide detailed L-shell and K-shell spectra in the 4 – 25 Å region (Brown et al. 1999). A flat-field spectrometer with either a 1200 $\ell$/mm or 2400 $\ell$/mm grating is used to study the 10 – 400 Å extreme ultraviolet region (Beiersdorfer et al. 1999b). A seventh port on the top of EBIT permits axial access to the trap and is used for the injection of singly charged metal ions into the trap from a metal vapor vacuum arc source.

A very important feature of using EBIT is the ability to produce ions of a desired charge state and study their emission by selecting specific line formation processes. To do so, we rely on the fact that we can choose the energy of the electron beam within about 30 eV. This provides us with a powerful technique to determine which line comes from which ionization state. A calculation of the iron ionization balance as a function of electron beam energy based on electron-impact ionization and radiative recombination is shown in Figure 2. In actuality, this distribution is somewhat smeared out because of charge transfer reactions between the trapped ions and background neutrals. Figure 3 illustrates the charge state selectivity given by proper choice of the electron beam energy. The spectrum in *(a)* shows the $2p - 3s$ emission lines in Fe XVII observed when the beam energy is 1200 eV. This energy is below the 1250-eV ionization potential of Fe XVII and only lines from Fe XVII are seen. The spectrum in *(b)* is obtained at 1300 eV, i.e., 50 eV higher than the ionization potential of Fe XVII. Consequently, Fe XVIII ions are produced. Comparing the two spectra allows us to unambiguously identify the transition at 17.623 Å as a transition in Fe XVIII. This particular line was observed in solar spectra and for some time was thought to result from inner-shell ionization by coronal X-rays and subsequent L-shell fluorescence of neutral and once ionized iron in the photosphere, as described by Drake et al. (1999).

In Figure 3*c* we show a spectrum of the Rydberg transitions of O VII. The wavelengths of these transitions are well known, and we have used them as reference lines in our measurements of the iron lines. In fact, all of our spectral measurements in the EUV and X-ray region are calibrated *in situ* by recording lines from hydrogenlike or heliumlike reference lines whose wavelengths are accurately known.

Line identifications and wavelength measurements are best made by setting the energy of the electron beam

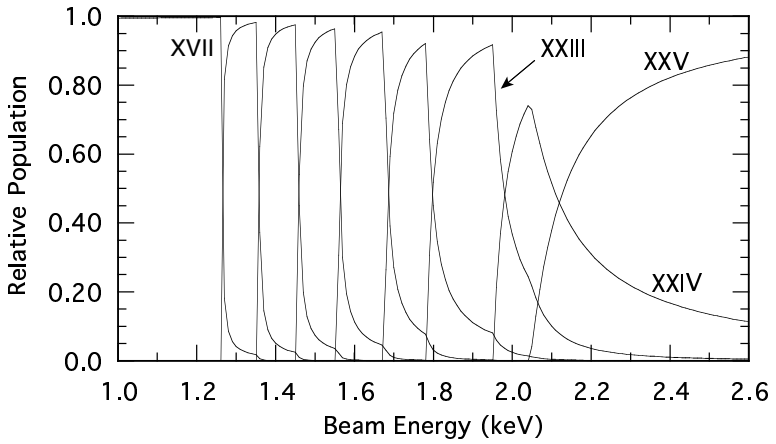


Fig. 2. Calculated iron ionization balance in EBIT as a function of electron beam energy.

Astrophysical Plasmas: Codes, Models, and Observations (Mexico City, 25-29 October 1999)
Editors: Jane Arthur, Nancy Brickhouse, & José Franco

to a constant value and integrating the resulting spectral emission over a given period of time. In contrast, excitation processes are best studied by sweeping the energy of the electron beam in a continuous fashion. Using an event-mode data acquisition system we tag each photon with the energy of the beam. The spectral data are then plotted as a function of electron beam energy. This allows us to determine the excitation function of a given spectral line. Resonant enhancement in the line emission, onsets of radiative cascades from higher levels, or dielectronic satellite features blending with a given line can thus be measured and the relative magnitude of each process assessed for different electron energies (cf. Section 5).

## 3. SPECTRAL CATALOGUES OF THE INTERMEDIATE CHARGE STATES OF IRON

The 30–140 Å region has never been systematically investigated in low-density laboratory plasmas. Moreover, the region has received incomplete attention in solar measurements. Consequently, many lines in this region have never been identified and are missing from present spectral models, as we have shown recently (Beiersdorfer et al. 1999a). This has hampered the correct interpretation of short-wavelength-band spectra from *EUVE*, causing a significant underestimation of the flux in this wavelength band (Schmitt, Drake, & Stern 1996; Drake, Laming, & Widing 1997). For example, we have measured a spectrum of Fe VII and Fe VIII, as shown in Figure 4. None of the observed lines in Fe VII and less than 75 % of the flux from lines in Fe VIII are in standard spectral modeling codes. The same is true for the emission lines from higher charge states of iron (Lepson et al. in these proceedings), e.g., more than 90 % of the flux from Fe XIII in the wavelength band below 140 Å is missing in the existing radiative loss models. As a result, the problems encountered in modeling the flux of the low charge states of iron in solar-like stellar coronae also pertain to the interpretation of spectra from coronae somewhat hotter than that of the Sun.

We have recently completed an inventory of all significant L-shell emission lines from Fe XVII through Fe XXIV in the 10 – 18 Å region (Brown et al. 1998; Phillips et al. 1999; Brown et al., in preparation). We found, for example, that the emission emanating from levels with high principal quantum number ($n \geq 5$) in Fe XVII equalled about 13 % of the flux of the strongest Fe XVII line. This is a significant amount of flux that is concentrated in a small wavelength band 0.5 Å wide near the Fe XVII ionization limit.

Overall, our measurements have yielded about twice as many lines as listed, for example, in the compilation by Kelly (1987).

## 4. CALIBRATION OF DIAGNOSTIC LINE RATIOS

The intensity ratio of the $3d \rightarrow 2p$ intercombination and resonance lines in Fe XVII at 15.014 and 15.261 Å respectively, has been proposed as a diagnotic of optical depth and hence of density in coronal active

Astrophysical Plasmas: Codes, Models, and Observations (Mexico City, 25-29 October 1999)
Editors: Jane Arthur, Nancy Brickhouse, & José Franco

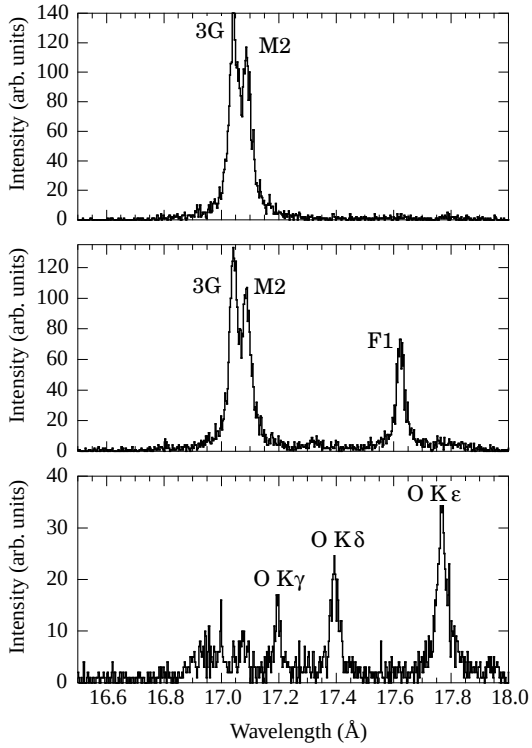


Fig. 3. Flat-crystal spectrometer spectra near 17 Å: *(a)* Fe XVII $2p-3s$ transitions measured at a beam energy of 1200 eV; *(b)* Fe XVIII line appears at 17.62 Å at a beam energy of 1300 eV; *(c)* O VII Rydberg transitions used for wavelength calibration.

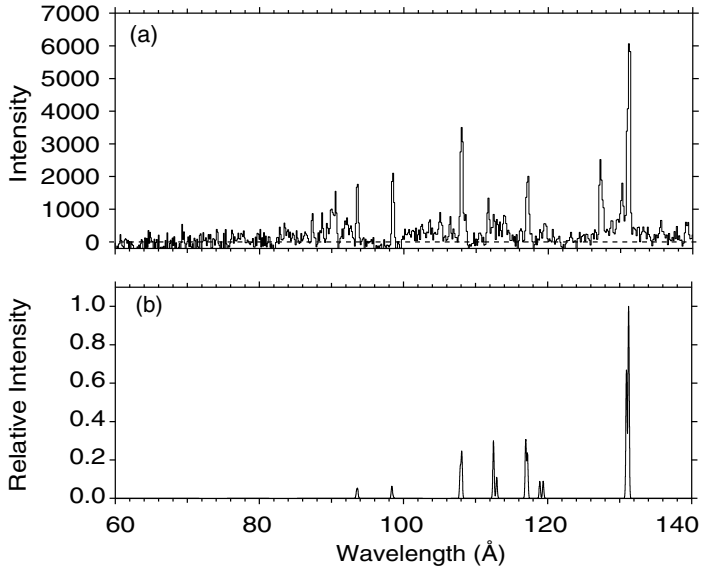


Fig. 4. Spectrum of Fe VII and Fe VIII in the extreme ultraviolet: *(a)* measurement on EBIT; *(b)* predictions from the MEKA model (Kaastra & Mewe 1993). The latter includes only lines from Fe VIII.

Astrophysical Plasmas: Codes, Models, and Observations (Mexico City, 25-29 October 1999)
Editors: Jane Arthur, Nancy Brickhouse, & José Franco

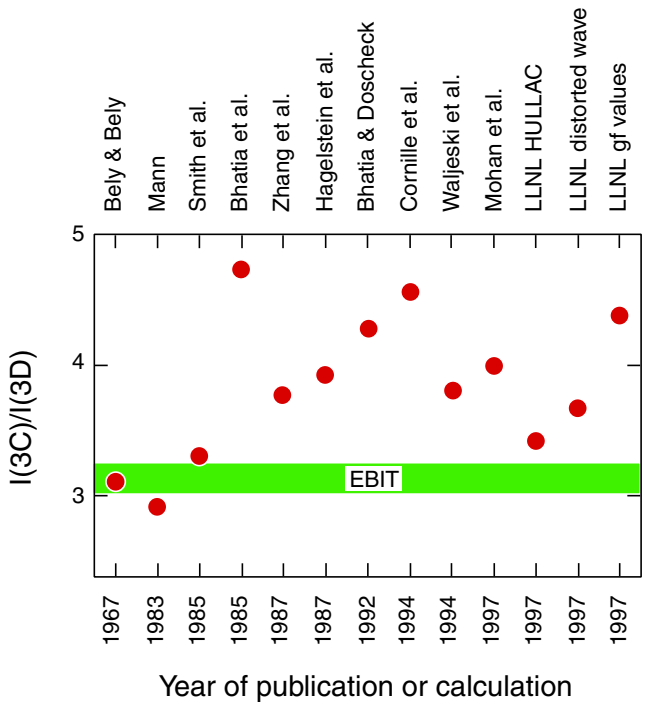


Fig. 5. Comparison of the predicted values (filled circles) for the optically thin ratio of the intensity of the $3d \rightarrow 2p$ resonance and intercombination lines in Fe XVII with the measured value shown as a horizontal band. The uncertainty of the measured value is indicated by the width of the band. The author(s) and year of publication of the prediction are given on the abscissa.

regions (Schmelz, Saba, & Strong 1992; Waljeski et al. 1994). Because the oscillator strength of the resonance line is much larger than that of the intercombination its observed emission can, under certain conditions, be significantly reduced in hot plasmas through resonance scattering of photons out of the line of sight (Rugge & McKenzie 1985). The use of this diagnostic to infer the optical depth is, however, impaired by the simple fact that modern calculations of electron-impact excitation cross sections are typically only accurate to between 5 and 30 %. In fact, a compilation of various predictions of the optically thin ratio based on different calculations shows scatter in the ratio from 2.9 to 4.7, as illustrated in Figure 5. Not knowing which calculation to use for the optical thin ratio, a measured ratio of 2.9, for example, may thus lead to an inferred optical depth between 0 and 3.

We have made a measurement of this ratio with EBIT and found a ratio of $3.03 \pm 0.12$ (Brown et al. 1998). This ratio agrees best with a prediction made by Bely & Bely (1967). This illustrates that the usual assumption that "the most recently published calculations are the best" is fallacious. On the other hand, the result does not imply that the atomic model used by Bely and Bely is superior to present-day calculations.

## 5. DIELECTRONIC RECOMBINATION CONTRIBUTIONS TO L-SHELL EMISSION LINES

Our measurements focus not only on line formation by electron-impact excitation but also on indirect line formation processes, such as those by resonance excitation and high-n dielectronic satellite contributions to L-shell emission lines (Gu et al. 1999). An example of the contributions from these processes to the line formation of a $3d \rightarrow 2p$ line in lithiumlike Fe XXIV is shown in Figure 6. The measurement clearly identifies the different contributions to the line: direct electron-impact excitation and resonance excitation above the threshold for excitation, and unresolved dielectronic-recombination satellite lines below threshold.

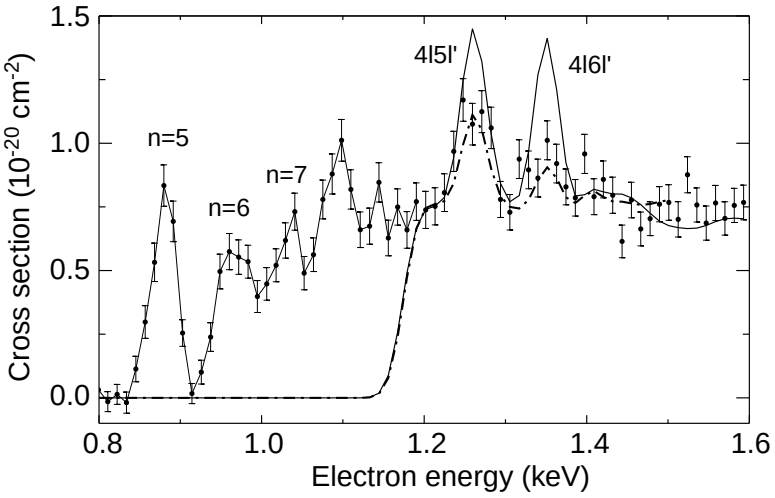


Fig. 6. Measured emission of the $3d_{5/2} \rightarrow 2p_{3/2}$ transition in lithiumlike $Fe^{23+}$ as a function of electron energy showing dielectronic satellite contributions below threshold and resonance excitation contributions above threshold for electron-impact excitation. Dotted line connects measured values; solid and dashed lines indicate predictions from two different models.

The contributions from the unresolved satellite lines are important for accounting for all of the flux of a given line. Calculations of the unresolved dielectronic satellites have not been carried out for most L-shell lines. Our measurements show that such satellites can enhance some L-shell lines in Fe XXIV by 20 % (Gu et al. 1999) or more, especially in colder plasmas. Such resonances may also affect the $3d \rightarrow 2p$ intercombination and resonance lines in Fe XVII, which we discussed above, and hence may change the inferred optical depths. In order to provide a complete accounting of all contributions to the flux of a given line, our current effort concentrates on measuring the dielectronic resonance contributions for all strong iron L-shell emission lines. The results of these measurements should be available in the near future.

## 6. CONCLUSION

We have presented several recent results of our ongoing laboratory effort to provide reliable atomic data for spectral modeling of astrophysical plasmas. The effort extends from compiling spectral catalogues to assessing line formation processes and calibrating diagnostic line ratios. By employing properly designed and executed measurements, our spectroscopic facility has become an analog computer where Nature computes the correct result for inclusion in spectral codes. With it we are able to address the issues of completeness and accuracy of the spectral models. Most importantly, the measurements provide uncertainty limits that are invaluable in establishing believable bounds on the physical parameters inferred from spectroscopic observations of astrophysical data.

This work was supported by NASA grants NAG5-6731 and NAG5-5123 and work order W-19127 and was performed under the auspices of the Department of Energy under contract No. W-7405-ENG-48.

## REFERENCES

Beiersdorfer, P., Bitter, M., von Goeler, S., & Hill, K. W. 1989a, Nucl. Instrum. Meth. B, 43, 347
Beiersdorfer, P., Lepson, J. K., Brown, G., Utter, S. B., Kahn, S., Liedahl, D., & Mauche, C. W. 1999a, ApJ, 519, L185
Beiersdorfer, P., López-Urrutia, J. R. C., Springer, P., Utter, S. B., & Wong, K. L. 1999b, Rev. Sci. Instrum., 70, 276

Astrophysical Plasmas: Codes, Models, and Observations (Mexico City, 25-29 October 1999)
Editors: Jane Arthur, Nancy Brickhouse, & José Franco

Beiersdorfer, P., Marrs, R. E., Henderson, J. R., Knapp, D. A., Levine, M. A., Platt, D. B., Schneider, M. B., Vogel, D. A., & Wong, K. L. 1990, Rev. Sci. Instrum., 61, 2338
Beiersdorfer, P., Osterheld, A., Phillips, T. W., Bitter, M., Hill, K. W., & von Goeler, S. 1995, Phys. Rev. E, 52, 1980
Beiersdorfer, P., Phillips, T., Jacobs, V. L., Hill, K. W., Bitter, M., von Goeler, S., & Kahn, S. M. 1993, ApJ, 409, 846
Beiersdorfer, P., von Goeler, S., Bitter, M., Hill, K., Hulse, R. A., & Walling, R. S. 1989b, Rev. Sci. Instrum., 60, 895
Bely, O., & Bely, F. 1967, Sol. Phys., 2, 285
Bitter, M., Hsuan, H., Hill, K. W., & Zarnstorff, M. 1993, Physica Scripta, T47, 87
Bombarda, F., Giannella, R., Källne, E., Tallents, G. J., Bely-Dubau, F., Faucher, P., Cornille, M., Dubau, J., & Gabriel, A. H. 1988, Phys. Rev. A, 37, 504
Brown, G., Beiersdorfer, P., Liedahl, D., Widmann, K., & Kahn, S., 1998, ApJ, 502, 1015
Brown, G. V., Beiersdorfer, P., & Widmann, K. 1999, Rev. Sci. Instrum., 70, 280
Decaux, V., Bitter, M., Hsuan, H., von Goeler, S., Hill, K. W., Hulse, R. A., Taylor, G., Park, H., & Bhalla, C. P. 1991, Phys. Rev. A, 43, 228
Drake, J. J., Laming, J. M., & Widing, K. G. 1997, ApJ, 478, 403-416.
Drake, J. J., Swartz, D. A., Beiersdorfer, P., Brown, G. V., & Kahn, S. M. 1999, ApJ, 521, 839
Gu, M., Kahn, S., Savin, D., Beiersdorfer, P., Brown, G., Liedahl, D., Reed, K., Bhalla, C., & Grabbe, S. 1999, ApJ, 518, 1002
Kaastra, J. S., & Mewe, R. 1993, Legacy, 3, 6
Keenan, F. P., McCann, S. M., Kingston, A. E., Barnsley, R., Dunn, J., & Peacock, N. J. 1991, Phys. Rev. A, 44, 3831
Kelly, R. L. 1987, J. Phys. Chem. Ref. Data, 16, Suppl. 1
Levine, M. A., et al. 1989, Nucl. Instrum. Methods, B43, 431
Phillips, K. J. H., Mewe, R., Harra-Murnion, L. K., Kaastra, J. S., Beiersdorfer, P., Brown, G. V., & Liedahl, D. A. 1999, A&AS, 138, 381
Rugge, H. R., & McKenzie, D. L. 1985, ApJ, 297, 338.
Schmelz, J. T., Saba, J. L. R., & Strong, K. T. 1992, ApJ, 398, L115.
Schmitt, J. H. M. M., Drake, J. J., & Stern, R. A. 1996, ApJ, 465, L51.
Smith, A. J., Bitter, M., Hsuan, H., Hill, K. W., von Goeler, S., Timberlake, J., Beiersdorfer, P., & Osterheld, A. 1993, Phys. Rev. A, 47, 3073
Stratton, B. C., Moos, H. W., & Finkenthal, M. 1984, ApJ, 279, L31
Sugar, J., & Rowan, R. L. 1995, J. Opt. Soc. Am. B, 12, 1403
Waljeski, K., Moses, D., Dere, K. P., Saba, J. L. R., Web, D. F., & Zarro, D. M. 1994, ApJ, 429, 909
Wargelin, B. J., Beiersdorfer, P., Liedahl, D. A., Kahn, S. M., & von Goeler, S. 1998, ApJ, 496, 1031

Astrophysical Plasmas: Codes, Models, and Observations (Mexico City, 25-29 October 1999)
Editors: Jane Arthur, Nancy Brickhouse, & José Franco

P. Beiersdorfer, G. V. Brown, D. A. Liedahl, C. Mauche, S. B. Utter: High Temperature Physics and Astrophysics Division, Lawrence Livermore National Laboratory, 7000 East Ave., Livermore, CA 94550, USA.
J. J. Drake, B. J. Wargelin: Harvard-Smithsonian Center for Astrophysics, 60 Garden Street, Cambridge, MA 02138, USA.
M.-F. Gu, S. M. Kahn, D. W. Savin: Department of Physics, Columbia University, 538 W 120th St., New York, NY 10027, USA.
J. K. Lepson: Space Sciences Laboratory, Univ. of California, Berkeley, CA 94720, USA.